The Journal of Nutrition
Nutritional Immunology

Galacto-oligosaccharides Protect the Intestinal Barrier by Maintaining the Tight Junction Network and Modulating the Inflammatory Responses after a Challenge with the Mycotoxin Deoxynivalenol in Human Caco-2 Cell Monolayers and B6C3F$_1$ Mice[1–3]

Peyman Akbari,[4,5] Saskia Braber,[4]* Arash Alizadeh,[4,5] Kim AT Verheijden,[5] Margriet HC Schoterman,[6] Aletta D Kraneveld,[5] Johan Garssen,[5,7] and Johanna Fink-Gremmels[4]

Divisions of [4]Veterinary Pharmacy, Pharmacology, and Toxicology, and [5]Pharmacology, Utrecht Institute for Pharmaceutical Sciences, Faculty of Science, Utrecht University, Utrecht, The Netherlands; [6]FrieslandCampina, Amersfoort, The Netherlands; and [7]Nutricia Research, Utrecht, The Netherlands

Abstract

Background: The integrity of the epithelial layer in the gastrointestinal tract protects organisms from exposure to luminal antigens, which are considered the primary cause of chronic intestinal inflammation and allergic responses. The common wheat-associated fungal toxin deoxynivalenol acts as a specific disruptor of the intestinal tight junction network and hence might contribute to the pathogenesis of inflammatory bowel diseases.

Objective: The aim of the current study was to assess whether defined galacto-oligosaccharides (GOSs) can prevent deoxynivalenol-induced epithelial dysfunction.

Methods: Human epithelial intestinal Caco-2 cells, pretreated with different concentrations of GOSs (0.5%, 1%, and 2%) for 24 h, were stimulated with 4.2-μM deoxynivalenol (24 h), and 6/7-wk-old male B6C3F$_1$ mice were fed a diet supplemented with 1% GOSs for 2 wk before being orally exposed to deoxynivalenol (25 mg/kg body weight, 6 h). Barrier integrity was determined by measuring transepithelial electrical resistance (TEER) and intestinal permeability to marker molecules. A calcium switch assay was conducted to study the assembly of epithelial tight junction proteins. Alterations in tight junction and cytokine expression were assessed by quantitative reverse transcriptase-polymerase chain reaction, Western blot analysis, or ELISA, and their localization was visualized by immunofluorescence microscopy. Sections of the proximal and distal small intestine were stained with hematoxylin/eosin for histomorphometric analysis.

Results: The in vitro data showed that medium supplemented with 2% GOSs improved tight junction assembly reaching an acceleration of 85% after 6 h ($P < 0.05$). In turn, GOSs prevented the deoxynivalenol-induced loss of epithelial barrier function as measured by TEER (114% of control), and paracellular flux of Lucifer yellow (82.7% of prechallenge values, $P < 0.05$). Moreover, GOSs stabilized the expression and cellular distribution of claudin3 and suppressed by >50% the deoxynivalenol-induced synthesis and release of interleukin-8 [IL8/chemokine CXC motif ligand (CXCL8)] ($P < 0.05$). In mice, GOSs prevented the deoxynivalenol-induced mRNA overexpression of claudin3 ($P = 0.022$) and *CXCL8* homolog keratinocyte hemoattractant (*Kc*) (*Cxcl1*) ($P = 0.06$) as well as the deoxynivalenol-induced morphologic defects.

Conclusions: The results demonstrate that GOSs stimulate the tight junction assembly and in turn mitigate the deleterious effects of deoxynivalenol on the intestinal barrier of Caco-2 cells and on villus architecture of B6C3F$_1$ mice. *J Nutr* 2015;145:1604–13.

Keywords: galacto-oligosaccharides, tight junction proteins, CXCL8, Caco-2 cells, intestinal integrity, deoxynivalenol

Introduction

The major function of the intestinal barrier is to protect the organism against invading bacterial and viral pathogens and food-borne toxins (1, 2). Defects in intestinal barrier function result in a paracellular influx of luminal antigens, which is considered a pivotal pathogenic factor in the onset and promotion of intestinal inflammation and inflammatory bowel diseases as well as allergies (3).

A dietary component that is known to affect the intestinal barrier function is the mycotoxin deoxynivalenol (4–8). Deoxynivalenol is one of the most frequently occurring natural toxins in

Manuscript received December 29, 2014. Initial review completed January 29, 2015. Revision accepted May 8, 2015.
First published online May 27, 2015; doi:10.3945/jn.114.209486.

wheat and wheat-based products and can readily enter the food and feed chain because deoxynivalenol is resistant to processing and heating (9). Consumption of foodstuffs contaminated by deoxynivalenol have been associated with human and animal intoxications, and the proinflammatory and immunotoxic effects of deoxynivalenol are of increasing concern for farm animals, such as pigs, as well as for humans (10–14). Human exposure to deoxynivalenol can cover all age groups, even the developing fetus, because it also transfers across the placental barrier (15, 16). Therefore, it is an important human safety issue, and these epidemiologic findings warrant the search for dietary supplements that can be used in infants and adults for the mitigation of the adverse effects of deoxynivalenol on intestinal integrity.

The gut health-promoting effects of nondigestible oligosaccharides have been broadly acknowledged (17). In particular, selected fractions of milk-derived galacto-oligosaccharides (GOSs)[8] are of interest because of their potential immunomodulatory and anti-inflammatory effects. GOSs, which resemble oligosaccharides that occur naturally in human breast milk, are currently used in infant formulas (18). They are expected not only to modulate the composition and metabolism of the gut microbiota by increasing Bifidobacteria and *Lactobacillus* spp. numbers (19–21), but seem to prevent specific pathologies involving the gut immune system, such as food allergies and inflammatory bowel disease, as demonstrated in clinical trials (19, 22, 23). However, the exact mechanisms involved in such immunomodulatory effects remain to be elucidated.

The aim of the current experiments was to characterize the effects of GOSs on the epithelial barrier with use of a standardized Caco-2 cell model and to investigate whether a potential barrier-stabilizing effect also results in improved integrity of the intestinal barrier function and reduced inflammatory response during a deoxynivalenol challenge.

Methods

GOS

GOSs are generally defined as a mixture of those substances produced from lactose by the enzyme β-galactosidase, comprising between 2 and 8 saccharide units (degree of polymerization), with one of these units being a terminal glucose and the remaining saccharide units being galactose and disaccharides composing 2 units of galactose (24, 25). For the current experiments, the commercial product Vivinal GOS syrup (FrieslandCampina Domo), containing ~45% GOSs with a degree of polymerization of 2–8, 16% free lactose, 14% glucose, and 25% water, was used. Dilutions (0.5%, 1%, and 2% GOSs) were made in complete cell culture medium. Before the functional assays described below, the potential cytotoxicity of GOSs at different concentrations for Caco-2 cells was measured by the Alamar Blue assay (Invitrogen), a standard method to assess cell viability. These control experiments confirmed that GOSs did not induce any cytotoxicity in Caco-2 cells at the selected test concentrations. In addition, close to equimolar concentrations of lactose (16%) and glucose (14%) present in the 2% GOS solution were included in the Caco-2 cell assays and had no effect on the deoxynivalenol-induced transepithelial electrical resistance (TEER) decrease and increase in paracellular flux of Lucifer yellow (LY) (**Supplemental Figure 1**).

Deoxynivalenol

Purified deoxynivalenol (D0156; Sigma) was diluted in absolute ethanol (99.9%; JT Baker) to prepare a 25-mM stock solution and was stored at −20°C. For the cell culture experiments, deoxynivalenol was diluted to a concentration of 4.2-μM deoxynivalenol in complete cell culture medium and added for the challenge experiments to the apical side as well as to the basolateral side of the transwell plates for 24 h. This deoxynivalenol concentration was selected on the basis of our previous results and did not impair cell viability (8). Physicochemical interactions between deoxynivalenol and GOSs were excluded by co-incubation experiments with both compounds because the free deoxynivalenol fraction remained unchanged as measured by standard HPLC analysis with affinity column clean up, based on the method described by Dombrink-Kurtzman et al. (26) (**Supplemental Figure 2**).

In vitro experiments

The Caco-2 cell model. Human epithelial colorectal adenocarcinoma (Caco-2) cells obtained from the American Type Tissue Collection (Code HTB-37) (Manassas, Virginia, passages 102–114) were used according to established methods, also described by Akbari et al. (8). In brief, cells were cultured in DMEM and seeded at a density of 0.3×10^5 cells into 0.3-cm^2 high-pore density (0.4 μm) inserts with a polyethylene terephthalate membrane (BD Biosciences) placed in a 24-well plate. The Caco-2 cells were maintained in a humidified atmosphere of 95% air and 5% CO_2 at 37°C. After 17–19 d of culturing, a confluent monolayer was obtained with a mean TEER exceeding 400 $\Omega \cdot cm^2$ measured by a Millicell-Electrical Resistance System voltohmmeter (Millipore).

The Caco-2 cells were preincubated with different concentrations of GOSs (0.5%, 1%, and 2%) for 24 h before being exposed to deoxynivalenol in the presence of GOSs for another 24 h. GOSs and deoxynivalenol were added to both compartments (apical and basolateral) of the transwell insert unless otherwise stated.

Additional experiments with Caco-2 cells were conducted in which *1*) GOSs were only added to the apical compartment, *2*) GOSs (apical and basolateral) were removed after 24-h pretreatment and before the cells were challenged with deoxynivalenol in GOS-free DMEM medium, and *3*) GOSs (apical and basolateral) was co-incubated with deoxynivalenol for 24 h (without preincubation with GOSs).

TEER measurements were conducted 24 h after deoxynivalenol incubation, and thereafter, the paracellular flux was measured with use of 2 different membrane-impermeable marker molecules: LY (0.457 kDa) and fluorescein isothiocyanate-dextran (FITC-dextran; 4 kDa) (Sigma) added at a concentration of 16 μg/mL to the apical side (350 μl) in the transwell plate for 4 h (8). Medium without fluorescent marker molecules was used as a blank, and the concentration of LY and FITC-dextran at the basolateral side was calculated on the basis of a standard curve in the concentration range of 0.19–12.5 μg marker molecule/mL.

Calcium switch assay. Caco-2 cells grown on inserts were pretreated with different concentrations of GOSs (0.5%, 1%, and 2%) either on the apical side or on both sides of the transwell inserts for 24 h, as described above. Subsequently, Caco-2 cells were deprived from calcium by washing the cells twice with prewarmed PBS and exposing the cells transiently for 20 min to 2-mM ethylene glycol-bis(2-aminoethyl ether)N,N,N′,N′-tetraacetic acid (EGTA) (Sigma) in calcium- and magnesium-free HBSS (Gibco; Invitrogen). At the end of the incubation period, HBSS-EGTA was removed and the cells were rinsed and allowed to recover in either complete cell culture DMEM (containing 2-mM $CaCl_2$) or in DMEM

[1] Supported by the European Union, European Regional Development Fund; the Ministry of Economic Affairs, Agriculture, and Innovation; Peaks in the Delta; the Municipality of Groningen; the Provinces of Groningen, Fryslân, and Drenthe; the Dutch Carbohydrate Competence Center (CCC WP25; www.cccresearch.nl); Nutricia Research; and FrieslandCampina.

[2] Author disclosures: P Akbari, A Alizadeh, AD Kraneveld, and J Fink-Gremmels, no conflicts of interest. S Braber and KAT Verheijden received grants from the Carbohydrate Competence Center (CCC) program; J Garssen is associated with Nutricia Research and MHC Schoterman with FrieslandCampina, which are both industrial partners in the Dutch Carbohydrate Competence Center.

[3] Supplemental Figures 1–11 and Supplemental Tables 1 and 2 are available from the "Online Supporting Material" link in the online posting of the article and from the same link in the online table of contents at http://jn.nutrition.org.

[8] Abbreviations used: *ACTB,* β-actin; *CLDN1,* claudin1; *CLDN2,* claudin2; *CLDN3,* claudin3; *CLDN4,* claudin4; *Cxcl1,* keratinocyte hemoattractant (*Kc*); *Cxcl2,* macrophage inflammatory protein-2α (*Mip2*); *CXCL8,* chemokine CXC motif ligand; FITC-dextran, fluorescein isothiocyanate-dextran; GOS, galacto-oligosaccharide; *Ifng,* interferon-γ; LY, Lucifer yellow; *OCLN,* occludin; PGLYRP3, peptidoglycan recognition protein 3; TEER, transepithelial electrical resistance; *Tnfa,* tumor necrosis factor-α; *ZO1,* zona occludens protein-1; *ZO2,* zona occludens protein-2.

*To whom correspondence should be addressed. E-mail: S.Braber@uu.nl.

supplemented with the addition of different concentrations of GOSs (0.5%, 1%, and 2%). TEER was monitored at various time points (2, 4, 6, 8, 12, 24 h) during this recovery period as an index of tight junction reassembly and restoration of barrier function. The results are expressed as a percentage of initial value (27).

Tight junction proteins: mRNA expression, Western blot analysis, and cellular distribution. The levels of mRNA expression of the tight junction target genes in Caco-2 cells pretreated with different concentrations of GOSs for 24 h before exposed to deoxynivalenol (in presence of GOSs) for 6 h were measured by qRT-PCR. Cells were harvested and total RNA extraction, cDNA preparation, and qRT-PCR analysis were performed as described previously (8). Forward and reverse primers for claudin1 (*CLDN1*), claudin3 (*CLDN3*), and claudin4 (*CLDN4*), occludin (*OCLN*), and zona occludens protein-1 (*ZO1*) and zona occludens protein-2 (*ZO2*) (**Supplemental Table 1**) were designed by using the National Center for Biotechnology Information primer-Basic Local Alignment Search Tool and were manufactured commercially (Eurogentec). Specificity and efficiency of selected primers were confirmed by qRT-PCR analysis and dilution series of pooled cDNA at a temperature gradient (55–65°C) for primer-annealing and subsequent melting curve analysis. *GAPDH* and β-actin (*ACTB*) were used as reference genes, and the GeNorm software (version 3.5) was used to identify the most stable reference genes.

For Western blots, GOS-pretreated Caco-2 cells were exposed to deoxynivalenol for 24 h (in the presence of GOSs), and total protein extracts were prepared as described previously (8). Equal protein amounts were separated by SDS-PAGE and blotted onto polyvinylidene difluoride membranes. Rabbit anti-claudin3 (1:500; Invitrogen) or rabbit anti-β-actin (1:4000; Cell Signaling) served as primary antibodies for overnight incubations at 4°C, and horseradish peroxidase-conjugated goat anti-rabbit (1:2000; Dako) served as the secondary antibody applied for 2 h at room temperature. Blots were washed in PBS-tween, incubated in commercial enhanced chemiluminescence reagents (Amersham Biosciences), and exposed to photographic film and scanned on a GS710 calibrated imagine densitometer for quantification. The cellular localization of CLDN3 was assessed by immunofluorescence microscopy after staining with rabbit anti-claudin3 (1:50, 34–1700; Invitrogen) (8), followed by incubation with Alexa-Fluor conjugated secondary antibody (Invitrogen). Immunolocalization of CLDN3 was visualized, and images were taken with use of the confocal laser-scanning microscope Leica True Confocal Point Scanner with Spectral Detection-II (Leica Microsystems GmbH) with Leica Application Suite Advanced Fluorescence software.

IL-8 (chemokine CXC motif ligand): mRNA expression and secretion. In parallel to the experimental steps as described for the tight junction proteins above, the chemokine CXC motif ligand (*CXCL8*) mRNA expression was analyzed by qRT-PCR (see primer sequences in Supplemental Table 1), and release of CXCL8 from Caco-2 cells into the medium of the apical side as well as the basolateral side of the transwell insert was measured by ELISA with use of the Human IL-8 ELISA Set (BD Biosciences) according to manufacturer's instructions.

In vivo experiments

Mice. Male B6C3F$_1$ mice (n = 5/6 per group, 5/6 mice per cage), 6–7 wk old with a mean weight of 19.9 ± 0.32 g (Charles River Laboratories, Calco, Italy) were housed under controlled conditions in standard laboratory cages with sterilized woody-clean sawdust bedding (Technilab–BMI) and were acclimated to the environment for 2 wk. The room was maintained on a 12-h light-dark cycle at ~20.5°C with a relative humidity of ~61.5%. They consumed water ad libitum and commercial rodent diet (AIN-93G) (28). Mice were randomly distributed into different experimental groups. All in vivo experimental protocols were approved by the local Ethics Committee for Animal Experiments (Reference number: DEC 2012.III.02.012) and were performed in compliance with national and international guidelines on animal experimentation.

Diets and deoxynivalenol gavage. The experimental AIN-93G–based diets were composed and mixed with 1% GOSs (1-kg diet containing 22.22-g/kg Vivinal GOS syrup) by Research Diet Services. Carbohydrates in Vivinal GOSs were compensated isocalorically in the control diet by means of cellulose (for GOSs), lactose (for lactose), and dextrose (for glucose). The diet was checked for deoxynivalenol contamination by standard HPLC analyses with affinity column clean-up, based on the method described by Dombrink-Kurtzman et al. (26). None of experimental diets exceeded the detection limit of 10-μg deoxynivalenol per kg feed. The mice were fed the AIN-93G diet with or without 1% GOSs for 2 wk before being challenged with deoxynivalenol, given by oral gavage at a dose of 25-mg/kg body weight in 200-μL sterile PBS (29–31). Control mice received 200-μL sterile PBS. Six hours after the deoxynivalenol challenge, mice were killed by cervical dislocation, blood was obtained by heart puncture and collected in MiniCollect Z Serum Sep tubes (Greiner Bio-one), and different parts of the intestine were collected and preserved for mRNA isolation and histology. Weight gain was monitored throughout the experiment and no significant differences were recorded between control- and GOS-fed mice, except on day 12, when a slight but significant increase in weight gain was observed in the GOS-fed mice (**Supplemental Figure 3**). This slight increase in weight gain could be possibly related to the food intake; however, this was not determined in this study.

Intestinal specimen from mice used for isolation of mRNA and qRT-PCR analysis. For mRNA isolation, the mouse intestine was flushed with cold PBS and separated into different segments. These segments were defined as follows: proximal small intestine (~2 cm after the pylorus), middle small intestine (7–8 cm after the pylorus), distal small intestine (final 1 cm before the ileocecal junction), and cecum and colon (first 1 cm after cecum). These intestinal wall samples (~1 cm) were snap frozen in liquid nitrogen and stored at −80°C until RNA isolation. Total RNA extraction, cDNA preparation, and qRT-PCR analysis were performed as described previously (8). Primer sequences with corresponding annealing temperatures are listed in **Supplemental Table 2**.

Immunofluorescence staining of intestinal specimen of mice. Swiss rolls (32) of the distal small intestine were fixed in 10% formalin and embedded in paraffin. For antigen retrieval, the 5-μm sections were boiled in 10-mM citrate buffer (pH 6.0) for 10 min in a microwave. Rabbit anti-claudin3 (1:50, 34–1700; Invitrogen) was used as the first antibody, and after incubation, immunofluorescence staining was conducted as described above.

Histomorphometric analysis of intestinal specimen of mice. Sections of the proximal and distal small intestine were stained with hematoxylin/eosin according to standard procedures. Photomicrographs were taken with an Olympus BX50 microscope equipped with a Leica DFC 320 digital camera (magnification of 200×). The morphometric analysis of the sections was performed on 10 randomly selected, well-oriented villi and crypts per animal. A computerized microscope-based image analyzer (Cell^D; Olympus Europa GmbH) was used to determine histomorphometric markers: villus height (measured from the tip of the villus to the villus-crypt junction) and crypt depth (measured from the crypt-villus junction to the base of the crypt). These regions were manually defined for each villi (8).

Statistical analysis. Results of in vitro experiments were expressed as means ± SEMs of 3 independent experiments (n = 3), each performed in triplicate (3 wells/condition). Differences between groups of in vitro experiments were statistically determined by using one-factor ANOVA with a Bonferroni post hoc test. Additionally, two-factor ANOVA was used to compare the effects of 2% GOS treatment with and without deoxynivalenol exposure. Data of in vivo experiments were expressed as means ± SEMs, n = 5–6 mice/experimental group (with the exception of Supplemental Figure 3, weight gain, n = 11–12 mice/experimental group) and were statistically analyzed by using a two-factor ANOVA followed by a Bonferroni post hoc test. Results were considered statistically significant when $P < 0.05$. Analyses were performed by using GraphPad Prism (version 6.0) (GraphPad). The required sample size to achieve the given power was calculated with use of the program PS-Power and Sample Size Calculation based on previous research.

Results

GOSs prevent the deoxynivalenol-induced impairment of the Caco-2 cell monolayer integrity. As shown in **Figure 1**A, GOSs modulated the deoxynivalenol-induced decrease in TEER in a concentration-dependent manner, and pretreatment with 2% GOSs entirely prevented the loss of integrity ($P < 0.001$). In line with these results, the deoxynivalenol-induced increase in tracer transport (LY and FITC-dextran) was decreased by GOSs ($P < 0.001$ and $P < 0.01$, respectively) (Figure 1B, C). Because GOSs were applied to the apical and basolateral sites in these experiments, additional experiments were conducted in which GOSs were given only to the apical site, or removed during the deoxynivalenol challenge, as indicated in **Table 1**. Under these conditions, 2% GOSs induced a protective effect on the deoxynivalenol-induced impaired monolayer integrity, albeit less pronounced than in experiments where GOSs were present at both sites and during the entire exposure period (Table 1). Neither 0.5% GOSs nor 1% GOSs were effective (Table 1). Co-incubation of GOSs and deoxynivalenol (without preincubation with GOSs) for 24 h did not counteract the deoxynivalenol-induced intestinal barrier disruption as observed in TEER values and tracer transport (**Supplemental Figure 4**).

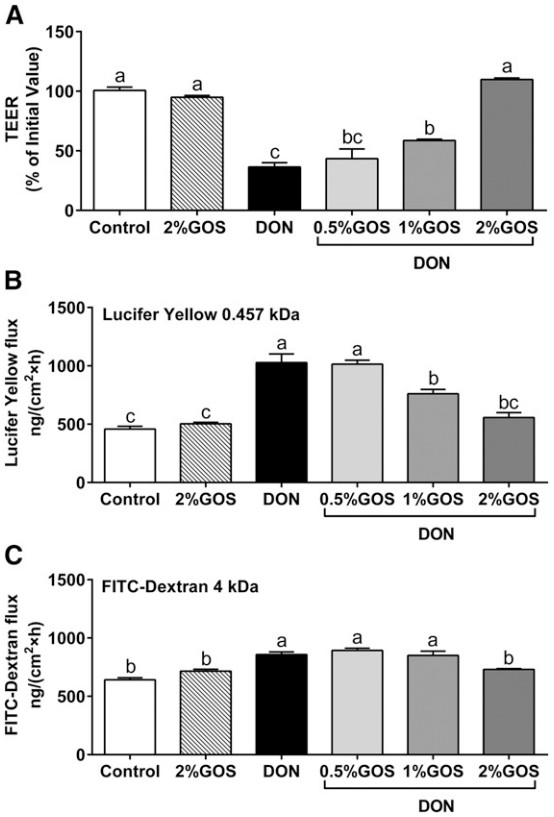

FIGURE 1 GOSs prevent the deoxynivalenol-induced impairment of the Caco-2 cell monolayer integrity. Caco-2 cells were pretreated apically and basolaterally with GOS or DMEM before the addition of deoxynivalenol (apical and basolateral compartments). TEER (A) and the transport of Lucifer yellow (B) and 4-kDa FITC-dextran (C) from the apical to the basolateral chamber were measured. Results are expressed as a percentage of initial value (TEER) or in the amount of tracer transported [ng/(cm^2 × h)] as means ± SEMs, $n = 3$. Labeled bars without a common letter differ, $P < 0.05$ (post hoc Bonferroni testing). DON, deoxynivalenol; FITC-dextran, fluorescein isothiocyanate-dextran; GOS, galacto-oligosaccharide; TEER, transepithelial electrical resistance.

GOSs accelerate tight junction reassembly after calcium deprivation in Caco-2 cells. It was demonstrated that GOSs caused a remarkable acceleration in tight junction reassembly over a period of 24 h (2% GOSs, 12 h; $P < 0.001$) (**Figure 2**). This effect remained when GOSs were removed during the recovery period (2% GOSs, 12 h; $P < 0.001$), and a significant acceleration in tight junction reassembly was also observed when GOSs were applied only at the apical site, albeit to a lesser degree (2% GOSs, 12 h; $P = 0.008$) (**Supplemental Figure 5**).

GOSs prevent the deoxynivalenol-induced disturbance of CLDN3 expression and its cellular distribution in Caco-2 cell monolayers. After a deoxynivalenol challenge of an established Caco-2 cell monolayer, mRNA expression levels of the tight junction proteins *CLDN3*, *CLDN4*, *OCLN*, *ZO1*, and *ZO2* were upregulated compared to the untreated cells (**Supplemental Figure 6**). Pretreatment with GOSs resulted in a less pronounced induction of *CLDN3* and this effect was statistically significant ($P = 0.022$) (**Figure 3**A). GOSs did not affect the deoxynivalenol-induced mRNA expression of *CLDN4*, *OCLN*, *ZO1*, and *ZO2* (Supplemental Figure 6). Subsequent Western blot analyses showed that deoxynivalenol induced a significant decrease in CLDN3 protein levels ($P = 0.006$), and this decrease was prevented by 2% GOSs ($P = 0.031$) (Figure 3B, C). Representative pictures of the CLDN3 cellular distribution of the Caco-2 monolayer are depicted in Figure 3D–F. Deoxynivalenol exposure was associated with a disturbed and irregular cellular distribution of CLDN3 and a translocation of CLDN3 from the cellular membrane to the submembraneous space (Figure 3E) compared to the control Caco-2 cells (Figure 3D). Control Caco-2 cells pretreated with GOSs did not affect the CLDN3 cellular distribution (data not shown), whereas the deoxynivalenol-induced deranged distribution of CLDN3 seemed to be prevented by GOSs (Figure 3F).

In vivo application of GOSs prevents the deoxynivalenol-induced overexpression of Cldn3 *mRNA and maintains its normal cellular distribution in mouse intestines.* The mRNA expression levels of claudin2 (*Cldn2*), *Cldn3*, and *Cldn4* were increased in a different pattern along the intestine after a deoxynivalenol challenge. The most pronounced effect was observed in the distal part of the small intestine (**Supplemental Figure 7**). *Zo1*, *Ocln*, and *Cldn1* remained unaffected in the different segments of the intestines of deoxynivalenol-exposed mice (Supplemental Figure 7). Interestingly, the deoxynivalenol-induced increase in *Cldn3* mRNA expression ($P = 0.004$) was significantly suppressed in the distal small intestine of mice fed a 1% GOS diet than a normal diet ($P = 0.024$) (**Figure 4**A). Additionally, a significant decrease in the deoxynivalenol-induced *Cldn2* mRNA expression was observed in the distal small intestine of mice fed a 1% GOS diet ($P = 0.018$). Dietary GOSs did not affect the deoxynivalenol-induced mRNA expression of investigated tight junction proteins in other segments than the distal small intestine (Supplemental Figure 7). To give an impression of the expression pattern of CLDN3 in the mouse distal small intestine, representative pictures of an immunofluorescence staining are shown in Figure 4B–D. In the distal small intestine of control mice, CLDN3 was located laterally between adjacent cells over the entire villus, with neither a specific signal at the apical surface nor on the basal membrane (Figure 4B), and this CLDN3 distribution pattern was also observed in the distal small intestine of control mice fed a GOS diet (data not shown). Deoxynivalenol exposure seemed to alter this typical CLDN3 distribution pattern toward an accumulation in the basal cytoplasm (Figure 4C). It seemed that the distribution of CLDN3 in the distal

TABLE 1 Apical and/or basolateral GOS exposure differently protect from the deoxynivalenol-induced impairment of the Caco-2 cell monolayer integrity[1]

	Route of GOS application					
	Apical and basolateral[2]		Apical[2]		Apical and basolateral[3]	
	TEER	LY flux	TEER	LY flux	TEER	LY flux
Control	101 ± 2.7[a]	458 ± 24[c]	103 ± 4.1[a]	261 ± 3.8[c]	94.5 ± 1.2[a]	305 ± 3.3[c]
2% GOSs	94.9 ± 1.5[a]	503 ± 12[c]	101 ± 3.3[a]	271 ± 13[c]	98.7 ± 1.7[a]	292 ± 32[c]
Deoxynivalenol	36.4 ± 3.6[c]	1027 ± 74[a]	36.0 ± 1.0[c]	761 ± 49[a]	22.4 ± 1.8[c]	1060 ± 65[a]
Deoxynivalenol + 0.5% GOSs	43.4 ± 8.1[b,c]	1014 ± 34[a]	40.9 ± 1.3[c]	618 ± 22[a,b]	23.1 ± 0.8[c]	1037 ± 86[a]
Deoxynivalenol + 1% GOSs	58.6 ± 1.0[b]	766 ± 38[b]	45.7 ± 1.5[b,c]	624 ± 29[a,b]	24.6 ± 0.7[c]	877 ± 35[a,b]
Deoxynivalenol + 2% GOSs	110 ± 1.2[a]	556 ± 42[b,c]	55.4 ± 1.0[b]	505 ± 49[b]	32.6 ± 1.6[b]	682 ± 28[b]
P	$P < 0.001$	$P < 0.001$	$P < 0.001$	$P < 0.001$	$P < 0.001$	$P < 0.001$

[1] Caco-2 cells were pretreated apically and basolaterally with GOSs (24 h) and then with deoxynivalenol (apical and basolateral compartments) plus GOSs (both apical and basolateral or only apical compartment) for another 24 h, or co-incubated apically and basolaterally with deoxynivalenol and GOSs for 24 h. TEER and LY flux are measured and results are expressed as a percentage of initial value (TEER) or amount of LY transported [ng/(cm^2 × h)] as means ± SEMs, $n = 3$. Means in a column without a common letter differ, $P < 0.05$ (post hoc Bonferroni testing). GOS, galacto-oligosaccharide; LY, Lucifer yellow; TEER, transepithelial electrical resistance.
[2] Duration of GOS application: 24-h preincubation with GOSs, 24-h co-incubation with GOS + deoxynivalenol.
[3] Duration of GOS application: 24-h preincubation with GOSs, 24-h incubation with deoxynivalenol.

small intestine of GOS-pretreated mice after deoxynivalenol exposure remained comparable to that of control mice (Figure 4D). Despite these effects of GOSs against the deoxynivalenol-induced overexpression of *Cldn3* mRNA and CLDN3 distribution, the deoxynivalenol-induced hyperpermeability of the intestines for FITC-dextran (4 kDa) ($P = 0.08$) was not mitigated in mice fed a 1% GOS diet than a normal diet (**Supplemental Figure 8**).

GOSs suppress the deoxynivalenol-induced increase in the mRNA expression as well as the synthesis and secretion of epithelial CXCL8 in Caco-2 cells. Deoxynivalenol induced an increase in mRNA expression levels of *CXCL8* ($P < 0.001$), and this effect was prevented by 1% and 2% GOS pretreatment as shown by a decrease in *CXCL8* mRNA levels ($P = 0.023$ and $P = 0.006$, respectively) (**Figure 5**A). Subsequent quantification of the secreted CXCL8 in the cell culture medium showed that 2% GOS pretreatment prevented the deoxynivalenol-induced increase in CXCL8 levels in both apical and basolateral chambers ($P < 0.001$ and $P = 0.002$, respectively) (Figure 5B, C).

*GOSs suppress the deoxynivalenol-induced increase in the expression of the murine CXCL8 analogs keratinocyte hemoattractant (*Kc*) and macrophage inflammatory protein-2α (*Mip2*) mRNA in the intestines.* The mRNA expression levels of different cytokines, such as interferon-γ (*Ifng*), *Il1a*, *Il1b*, *Il4*, *Il6*, tumor necrosis factor-α (*Tnfa*), and the murine *CXCL8* homologs, keratinocyte hemoattractant (*Kc*) (*Cxcl1*) and macrophage inflammatory protein-2α (*Mip2*) (*Cxcl2*), were measured in intestinal samples of deoxynivalenol-treated mice by qRT-PCR (**Supplemental Figure 9**). Only *Cxcl1* and *Cxcl2* mRNA expression was upregulated in the deoxynivalenol-exposed mouse intestines, especially in the small intestine, compared with the nontreated mice ($P = 0.042$ and $P = 0.026$, respectively), (**Supplemental Figure 10**). In the mice pretreated with GOSs, the deoxynivalenol-induced *Cxcl1* mRNA expression tended to be suppressed in the distal small intestine ($P = 0.06$) (Figure 5D, E).

GOSs prevent the deoxynivalenol-induced histomorphologic alterations in the mouse intestine. Deoxynivalenol-treated mice showed a significant decrease in villus height (**Figure 6**A) in the proximal small intestine than the nontreated mice ($P = 0.023$), whereas in the distal small intestine a slight decrease in villus height was observed after the deoxynivalenol gavage ($P < 0.08$) (Figure 6C). Offering the mice a diet supplemented with 1% GOSs before the deoxynivalenol challenge prevented these typical deoxynivalenol-induced histomorphologic changes in the proximal small intestine ($P = 0.032$) (Figure 6B, D). The crypt depth was significantly increased in the proximal small intestine in deoxynivalenol-treated mice than nontreated mice ($P = 0.022$), but GOSs did not affect this variable ($P = 0.57$) (**Supplemental Figure 11**).

Discussion

Nondigestible oligosaccharides are known to exert a beneficial effect on gut microbiota in infants and adults (19, 23) and are recommended as supportive therapy in patients with ulcerative colitis (22) and other chronic inflammatory conditions (17). Although the risk factors and pathogenesis of chronic inflammatory bowel diseases are still not entirely elucidated (33), several findings suggest a possible role for the wheat-associated mycotoxin deoxynivalenol in the induction and/or progression of human chronic intestinal inflammatory diseases (11, 34, 35). Given the global and frequent occurrence of deoxynivalenol, its stability during food processing, and its known toxic effects,

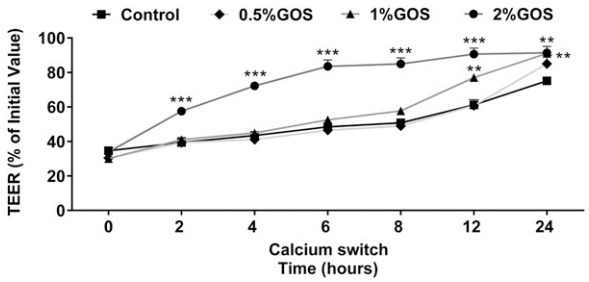

FIGURE 2 GOSs accelerate tight junction reassembly after calcium deprivation of Caco-2 cells. Caco-2 cells were pretreated apically and basolaterally with GOSs before calcium deprivation, and the TEER was measured during recovery (0, 2, 4, 6, 8, 12, and 24 h) in complete calcium-containing DMEM with GOSs. Results are expressed as a percentage of initial value as means ± SEMs, $n = 3$. **,***Significantly different from control at each independent time point (post hoc Bonferroni testing): $^{**}P < 0.01$, $^{***}P < 0.001$. GOS, galacto-oligosaccharide; TEER, transepithelial electrical resistance.

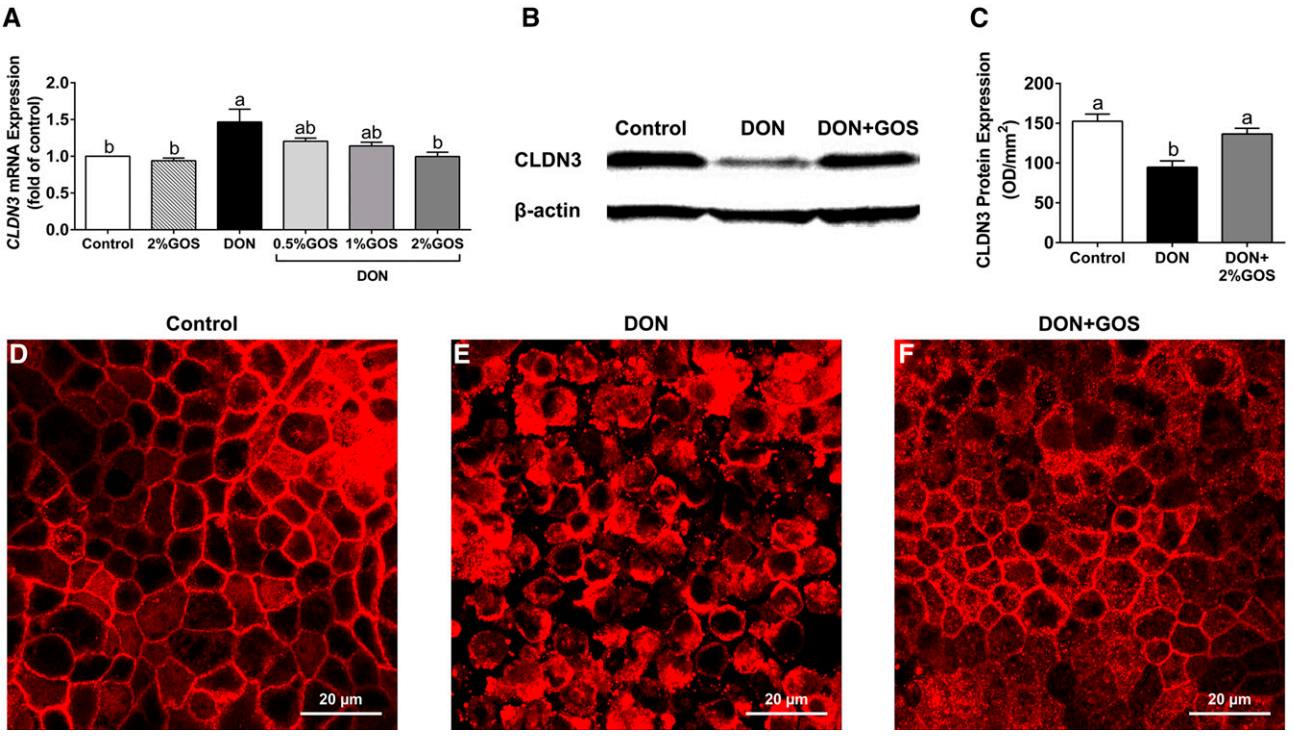

FIGURE 3 GOSs prevent the deoxynivalenol-induced disturbance of *CLDN3* expression and its cellular distribution in Caco-2 cell monolayers. *CLDN3* mRNA (A) and protein levels (B and C) after a deoxynivalenol challenge (apical and basolateral compartments) in Caco-2 cells apically and basolaterally pretreated with GOSs or DMEM. Results are expressed as *CLDN3* mRNA expression (fold of control) (qRT-PCR, normalized to *GAPDH* and *ACTB*) or CLDN3 protein expression (OD/mm^2) (Western blot, normalized to β-actin) as means ± SEMs, $n = 3$. Labeled bars without a common letter differ, $P < 0.05$ (post hoc Bonferroni testing). Immunofluorescence photomicrographs (D, E, and F) of Caco-2 monolayers stained with CLDN3 in the presence and absence of GOSs and deoxynivalenol. Representative results were reproduced in 3 separate experiments (400× magnification). *ACTB,* β-actin; *CLDN3,* claudin3; DON, deoxynivalenol; GOS, galacto-oligosaccharide.

deoxynivalenol is considered to be of public health concern as a food contaminant (9, 10, 36, 37). The aim of the current study was to assess the potential beneficial effects of defined GOSs on the deoxynivalenol-induced intestinal damage in a series of in vitro models and an in vivo study in mice. The presented in vitro results demonstrate the ability of GOSs to prevent the deoxynivalenol-induced loss of barrier function measured as transepithelial resistance and paracellular transport of marker molecules. Comparing the results of the various experimental approaches in which GOSs were added either to both the apical and basolateral site of the Caco-2 cell monolayer or to the apical site only, or simultaneously with deoxynivalenol (without a pretreatment phase), showed that the most pronounced effect was achieved when a pretreatment of GOSs added to both compartments was preceding the deoxynivalenol challenge. These findings suggest that GOSs have predominantly a preventive effect, although a more rapid repair of existing deoxynivalenol lesions cannot be excluded. The latter mechanism is suggested by the calcium switch assay, showing an acceleration of the tight junction assembly by GOSs and hence a decreased repair time of the transepithelial resistance after a calcium-deprivation period.

The difference between the results obtained with dual exposure of GOSs to the apical and basolateral compartment, which were more pronounced than an application to the apical compartment only, were unexpected because Gnoth et al. (38) and Eiwegger et al. (39) showed in vitro evidence for a transport of human milk oligosaccharides and prebiotic oligosaccharides, like GOSs, across the intestinal epithelial layer. These findings suggest an absorption of orally applied GOSs, which was recently supported by the presence of human milk oligosaccharides in the circulation (plasma and urine) of breastfed infants (40). A possible explanation for the different results in the current experiments regarding the route of GOS exposure could be the rather short preincubation time of 24 h, which might not be sufficient to allow an equilibrium between both compartments by means of transcellular transport of GOSs.

The direct effect of GOSs on tight junctions was further substantiated by the related gene expression profile of different tight junction proteins (*CLDN1*, *CLDN3*, *CLDN4*, *OCLN*, *ZO1*, and *ZO2*) in deoxynivalenol-exposed cells with or without GOS pretreatment. Only the deoxynivalenol-induced *CLDN3* mRNA expression could be almost entirely prevented by GOSs. Western blot analyses pointed out that GOS pretreatment also prevented the deoxynivalenol-induced decrease in CLDN3 protein expression. In addition, it seemed that the deoxynivalenol-induced derangement of the cellular distribution of CLDN3 was moderated by GOSs visualized by immunofluorescence microscopy. This contradiction between increase in tight junction mRNA expression and decrease in protein levels after deoxynivalenol exposure was earlier reported by De Walle et al. (41). Deoxynivalenol seems to prolong the usually transient expression of genes related to activation of signaling cascades by transcriptional enhancement and/or transcript stabilization (42). Conflicting results are described related to mechanisms behind the deoxynivalenol-related effect on claudins. Pinton et al. (43, 44) described that the deoxynivalenol-induced activation of the ERK signaling pathway inhibits CLDN4 protein expression, whereas others pointed out that extracellular signal-regulated

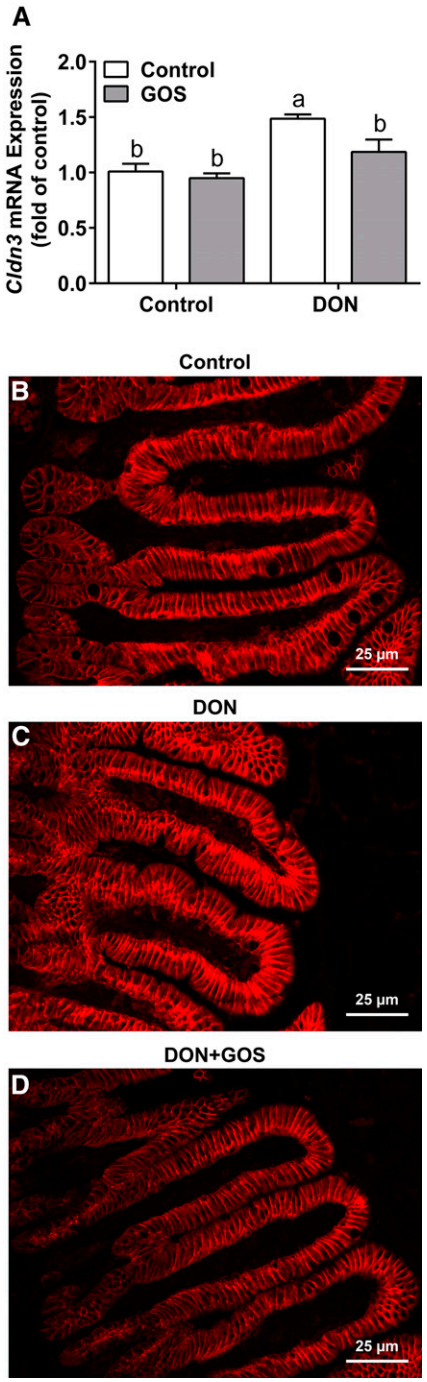

FIGURE 4 In vivo application of GOSs prevents the deoxynivalenol-induced overexpression of *Cldn3* mRNA and maintains its normal cellular distribution in mouse intestine. *Cldn3* mRNA levels (A) after a deoxynivalenol challenge in the distal small intestine of mice fed a diet that was or was not supplemented with GOSs. qRT-PCR data are normalized to *Gapdh* and *Actb* and expressed as *Cldn3* mRNA expression (fold of control) as means ± SEMs, n = 5–6 mice/experimental group. Labeled bars without a common letter differ, $P < 0.05$ (post hoc Bonferroni testing). Representative immunofluorescence photomicrographs (B, C, and D) of the mouse distal small intestine stained with CLDN3 (400× magnification). *Cldn3*, claudin3; DON, deoxynivalenol; GOS, galacto-oligosaccharide.

kinase, c-Jun N-terminal kinase, and NF-κB pathways were not involved (41). These findings suggest that deoxynivalenol is not solely reducing the tight-junction protein expression by inhibition of protein synthesis, but by a complex deregulation of gene expression and transcription pathways.

CLDN3 has previously been identified as one of the most affected tight junction proteins after deoxynivalenol exposure in intestinal porcine epithelial cells derived from jejunum (7) and Caco-2 cells (8), and the effect of deoxynivalenol on members of the claudin family has been also described in different in vivo studies (4, 8, 34, 41, 43, 44). Our in vitro results showing that GOSs counteracted the deoxynivalenol-induced disturbance of CLDN3 expression was confirmed in the in vivo mouse model. CLDN3 is strongly expressed in the mouse small intestine (45) and plays an important role in the postnatal maturation of murine intestinal barrier functions (46). In the current study, the induction of *Cldn3* mRNA expression in the distal small intestine after a deoxynivalenol challenge was shown to be prevented in mice pretreated with a GOS-supplemented diet. The mechanisms behind this effect await further clarification. Although CLDN3 is an important regulator of epithelial barrier permeability and seals the paracellular pathway against the passage of ions (47, 48), the deoxynivalenol-induced hyperpermeability of the intestines for FITC-dextran (4 kDa) was not mitigated by GOSs. A direct comparison between the in vitro findings and the findings in mice needs to consider the fact that in mice more important determinants of intestinal permeability are present, such as the mucous layer, secretory IgA, and distinct other cell types, including Goblet cells, Paneth cells, and immune cells, each of which contributes in a unique way to the maintenance of barrier integrity (49–52).

Previous investigations indicated that deoxynivalenol can induce both immunostimulatory or immunosuppressive responses depending on dose, frequency, and duration of exposure (10, 53), and hence, we studied some typical markers of intestinal inflammation. The chemokine CXCL8 is the most prominent cytokine expressed by Caco-2 cells and is secreted early in the inflammatory process by human enterocytes in vivo. It acts as a potent chemo-attractant for neutrophils, an effect that is also described after dietary deoxynivalenol exposure (35). The current study demonstrated that 1% and 2% GOSs prevent the deoxynivalenol-induced epithelial mRNA expression of *CXCL8* in Caco-2 cells. These findings are in line with previous results with oligosaccharides, in which it could be shown that α3-sialyllactose or fructo-oligosaccharides suppressed *CXCL8* mRNA expression levels in nonstimulated Caco-2 cells (54). The deoxynivalenol-induced CXCL8 release in both the apical and basolateral chamber was also counteracted by GOSs. Basolateral secretion of CXCL8 plays a role in the recruitment of circulating neutrophils from the bloodstream to site of tissue injury or infection, and it is speculated that apically secreted CXCL8 may initiate or augment the pathway responses in epithelial restitution before any potential loss of barrier integrity because of toxin production (55–58). Parallel to the in vitro experiments with human-derived Caco-2 cells, in the in vivo experiments with mice, the upregulation of the murine *CXCL8* homologs, *Cxcl1* and *Cxcl2*, by deoxynivalenol was noted, especially in the small intestine. The effect on *Cxcl1* in the distal small intestine could be alleviated by GOS pretreatment as well. Previously, it was suggested that GOSs interact with peptidoglycan recognition protein 3 (PGLYRP3) and PPARγ, carbohydrate receptors, such as C-type lectin and Toll-like receptor-4 that may contribute to the protective effects of GOSs (17, 54, 59).

In addition, the control conditions with GOSs did not affect the different markers measured in the Caco-2 cell model and in the in

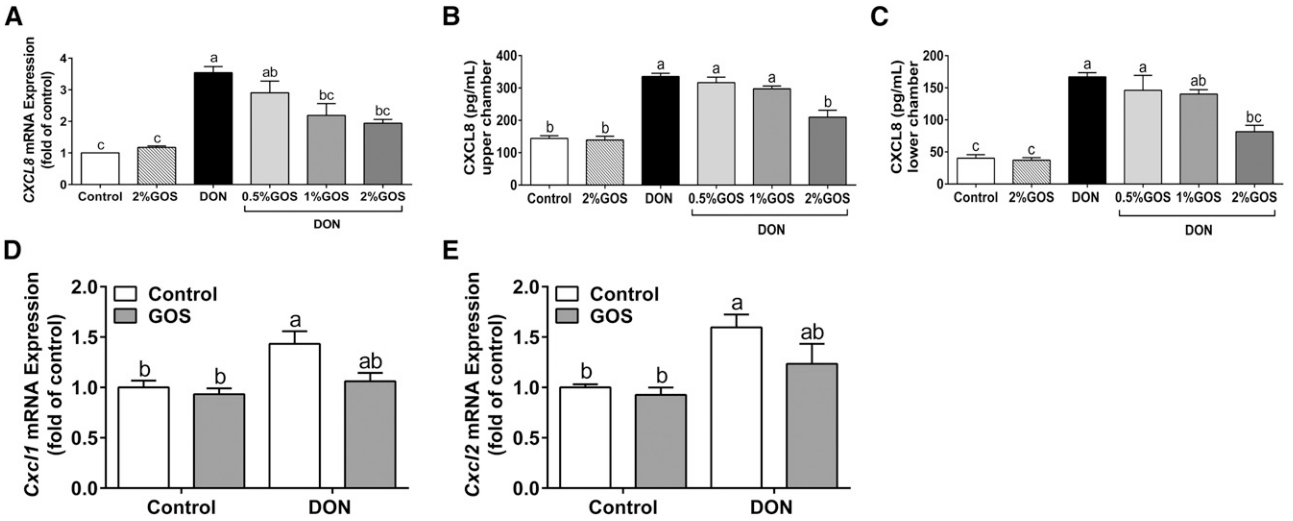

FIGURE 5 GOSs suppress the deoxynivalenol-induced changes in the expression, synthesis, and secretion of CXCL8 in Caco-2 cells as well as *Cxcl1* and *Cxcl2* mRNA expression in the mouse intestine. *CXCL8* mRNA (A) and protein levels (B and C) after a deoxynivalenol challenge (apical and basolateral compartments) in Caco-2 cells apically and basolaterally pretreated with GOSs or DMEM. *Cxcl1* and *Cxcl2* mRNA levels after a deoxynivalenol challenge in mice fed a diet that was or was not supplemented with GOSs (D and E). ELISA results are expressed as pg/mL as means ± SEMs, and qRT-PCR data are normalized to *Gapdh* and *Actb* and expressed as *CXCL8* and *Cxcl1*/*Cxcl2* mRNA expression (fold of control) as means ± SEMs, in vitro: $n = 3$ and in vivo: $n = 5$–6 mice/experimental group. Labeled bars without a common letter differ, $P < 0.05$ (post hoc Bonferroni testing). *Cxcl1*, keratinocyte hemoattractant (*Kc*); *Cxcl2*, macrophage inflammatory protein-2α (*Mip2*); *CXCL8*, chemokine CXC motif ligand; DON, deoxynivalenol; GOS, galacto-oligosaccharide.

vivo mouse model. Other in vitro and in vivo studies also described no effect in control conditions with GOSs in combination with fructo-oligosaccharides (60–63), and this could be related to the difficulty to positively affect the homeostatic environment.

In summary, the presented in vitro and in vivo studies demonstrated that GOSs, in a concentration-dependent manner, are able to prevent typical adverse effects of the wheat-derived fungal toxin deoxynivalenol. Of particular interest is the effect of GOSs on facilitating tight junction assembly and on the regulation of CLDN3 expression. Moreover, a reduction of the inflammatory response (CXCL8 and *Cxcl1*) after a deoxynivalenol challenge could be observed in line with a prevention of deoxynivalenol-induced alterations in villus architecture in the mouse intestine. Considering that the deoxynivalenol-induced alterations in the intestinal tract resemble those of human chronic inflammatory diseases (64–66) and the regular exposure of humans to deoxynivalenol because of its presence in wheat and wheat-derived products, further studies are warranted to assess in more detail the potential beneficial effects of GOSs as supportive therapy in the prevention of toxin-induced inflammatory bowel diseases and related syndromes.

Acknowledgments

PA conducted the research, analyzed the data, performed the statistical analysis, and wrote the paper; SB designed and conducted the research and wrote the paper; AA provided technical support for the in vitro experiments; KATV provided technical support for the in vivo experiments; MHCS and JG provided essential reagents or materials; MHCS and ADK provided critical revision of the manuscript; JG provided interpretation of the data; and JF-G designed the research objectives and had responsibility for the final content of the manuscript. All authors read and approved the final manuscript.

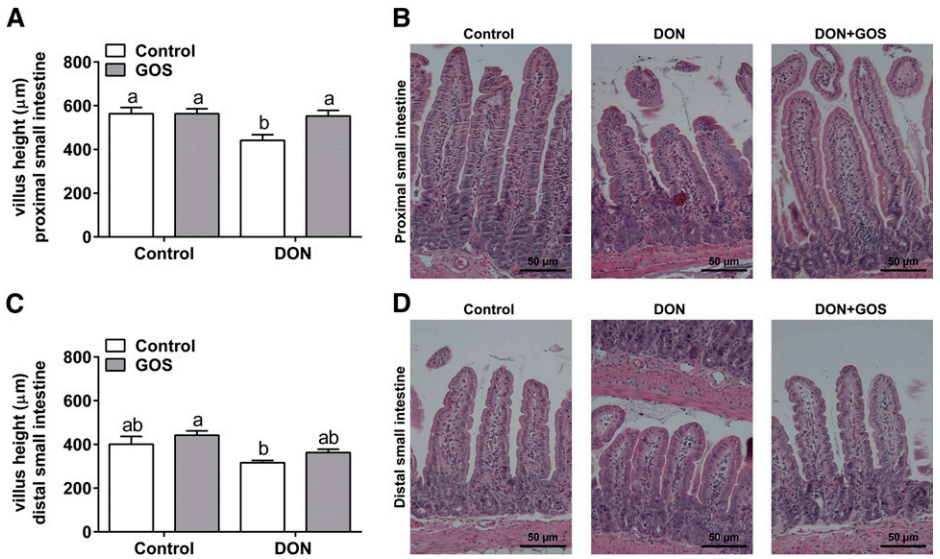

FIGURE 6 GOSs prevent the deoxynivalenol-induced histomorphologic alterations in the villi of the mouse intestine. Villus height in proximal (A) and distal (C) small intestine with representative photomicrographs of H&E-stained tissue (B, D) after a deoxynivalenol challenge in mice fed a diet that was or was not supplemented with GOSs (200× magnification). Results are expressed as means ± SEMs, $n = 5$–6 mice/experimental group. Labeled bars without a common letter differ, $P < 0.05$ (post hoc Bonferroni testing). DON, deoxynivalenol; GOS, galacto-oligosaccharide; H&E, hematoxylin/eosin.

References

1. Camilleri M, Madsen K, Spiller R, Greenwood-Van Meerveld B, Verne GN. Intestinal barrier function in health and gastrointestinal disease. Neurogastroenterol Motil 2012;24:503–12. Erratum in: Neurogastroenterol Motil 2012;24:976.
2. Ménard S, Cerf-Bensussan N, Heyman M. Multiple facets of intestinal permeability and epithelial handling of dietary antigens. Mucosal Immunol 2010;3:247–59.
3. Groschwitz KR, Hogan SP. Intestinal barrier function: molecular regulation and disease pathogenesis. J Allergy Clin Immunol 2009;124:3–20.
4. Pinton P, Tsybulskyy D, Lucioli J, Laffitte J, Callu P, Lyazhri F, Grosjean F, Bracarense AP, Kolf-Clauw M, Oswald IP. Toxicity of deoxynivalenol and its acetylated derivatives on the intestine: differential effects on morphology, barrier function, tight junction proteins, and mitogen-activated protein kinases. Toxicol Sci 2012;130:180–90.
5. Nossol C, Diesing AK, Kahlert S, Kersten S, Kluess J, Ponsuksili S, Hartig R, Wimmers K, Danicke S, Rothkotter HJ. Deoxynivalenol affects the composition of the basement membrane proteins and influences en route the migration of CD16(+) cells into the intestinal epithelium. Mycotoxin Res 2013;29:245–54.
6. Devreese M, Pasmans F, De Backer P, Croubels S. An in vitro model using the IPEC-J2 cell line for efficacy and drug interaction testing of mycotoxin detoxifying agents. Toxicol In Vitro 2013;27:157–63.
7. Diesing AK, Nossol C, Danicke S, Walk N, Post A, Kahlert S, Rothkotter HJ, Kluess J. Vulnerability of polarised intestinal porcine epithelial cells to mycotoxin deoxynivalenol depends on the route of application. PLoS ONE 2011;6:e17472.
8. Akbari P, Braber S, Gremmels H, Koelink PJ, Verheijden KA, Garssen J, Fink-Gremmels J. Deoxynivalenol: a trigger for intestinal integrity breakdown. FASEB J 2014;28:2414–29.
9. Sugita-Konishi Y, Park BJ, Kobayashi-Hattori K, Tanaka T, Chonan T, Yoshikawa K, Kumagai S. Effect of cooking process on the deoxynivalenol content and its subsequent cytotoxicity in wheat products. Biosci Biotechnol Biochem 2006;70:1764–8.
10. Pestka JJ. Deoxynivalenol: mechanisms of action, human exposure, and toxicological relevance. Arch Toxicol 2010;84:663–79.
11. Cano PM, Seeboth J, Meurens F, Cognie J, Abrami R, Oswald IP, Guzylack-Piriou L. Deoxynivalenol as a new factor in the persistence of intestinal inflammatory diseases: an emerging hypothesis through possible modulation of Th17-mediated response. PLoS ONE 2013;8:e53647.
12. Pestka JJ. Deoxynivalenol: toxicity, mechanisms and animal health risks. Anim Feed Sci Technol 2007;137:283–98.
13. Pinton P, Oswald IP. Effect of deoxynivalenol and other type B trichothecenes on the intestine: a review. Toxins (Basel) 2014;6:1615–43.
14. Larsen JC, Hunt J, Perrin I, Ruckenbauer P. Workshop on trichothecenes with a focus on DON: summary report. Toxicol Lett 2004;153:1–22.
15. Dänicke S, Brussow KP, Goyarts T, Valenta H, Ueberschar KH, Tiemann U. On the transfer of the Fusarium toxins deoxynivalenol (DON) and zearalenone (ZON) from the sow to the full-term piglet during the last third of gestation. Food Chem Toxicol 2007;45:1565–74.
16. Nielsen JK, Vikstrom AC, Turner P, Knudsen LE. Deoxynivalenol transport across the human placental barrier. Food Chem Toxicol 2011;49:2046–52.
17. Vos AP, M'Rabet L, Stahl B, Boehm G, Garssen J. Immune-modulatory effects and potential working mechanisms of orally applied non-digestible carbohydrates. Crit Rev Immunol 2007;27:97–140.
18. Sangwan V, Tomar SK, Singh RR, Singh AK, Ali B. Galactooligosaccharides: novel components of designer foods. J Food Sci 2011;76:R103–11.
19. Vulevic J, Drakoularakou A, Yaqoob P, Tzortzis G, Gibson GR. Modulation of the fecal microflora profile and immune function by a novel trans-galactooligosaccharide mixture (B-GOS) in healthy elderly volunteers. Am J Clin Nutr 2008;88:1438–46.
20. Fanaro S, Marten B, Bagna R, Vigi V, Fabris C, Pena-Quintana L, Arguelles F, Scholz-Ahrens KE, Sawatzki G, Zelenka R, et al. Galacto-oligosaccharides are bifidogenic and safe at weaning: a double-blind randomized multicenter study. J Pediatr Gastroenterol Nutr 2009;48:82–8.
21. Ben XM, Zhou XY, Zhao WH, Yu WL, Pan W, Zhang WL, Wu SM, Van Beusekom CM, Schaafsma A. Supplementation of milk formula with galacto-oligosaccharides improves intestinal micro-flora and fermentation in term infants. Chin Med J (Engl) 2004;117:927–31.
22. Ishikawa H, Matsumoto S, Ohashi Y, Imaoka A, Setoyama H, Umesaki Y, Tanaka R, Otani T. Beneficial effects of probiotic bifidobacterium and galacto-oligosaccharide in patients with ulcerative colitis: a randomized controlled study. Digestion 2011;84:128–33.
23. Fanaro S, Boehm G, Garssen J, Knol J, Mosca F, Stahl B, Vigi V. Galacto-oligosaccharides and long-chain fructo-oligosaccharides as prebiotics in infant formulas: a review. Acta Paediatr Suppl 2005;94:22–6.
24. Torres DPM, Goncalves MP, Teixeira JA, Rodrigues LR. Galacto-oligosaccharides: production, properties, applications, and significance as prebiotics. Comprehensive Reviews in Food Science and Food Safety 2010;9:438–54.
25. Coulier L, Timmermans J, Bas R, Van Den Dool R, Haaksman I, Klarenbeek B, Slaghek T, Van Dongen W. In-depth characterization of prebiotic galacto-oligosaccharides by a combination of analytical techniques. J Agric Food Chem 2009;57:8488–95.
26. Dombrink-Kurtzman MA, Poling SM, Kendra DF. Determination of deoxynivalenol in infant cereal by immunoaffinity column cleanup and high-pressure liquid chromatography-UV detection. J Food Prot 2010;73:1073–6.
27. Artursson P, Magnusson C. Epithelial transport of drugs in cell culture. II: Effect of extracellular calcium concentration on the paracellular transport of drugs of different lipophilicities across monolayers of intestinal epithelial (Caco-2) cells. J Pharm Sci 1990;79:595–600.
28. Reeves PG, Nielsen FH, Fahey GC, Jr. AIN-93 purified diets for laboratory rodents: final report of the American Institute of Nutrition ad hoc writing committee on the reformulation of the AIN-76A rodent diet. J Nutr 1993;123:1939–51.
29. Kinser S, Li M, Jia Q, Pestka JJ. Truncated deoxynivalenol-induced splenic immediate early gene response in mice consuming (n-3) polyunsaturated fatty acids. J Nutr Biochem 2005;16:88–95.
30. Moon Y, Pestka JJ. Cyclooxygenase-2 mediates interleukin-6 upregulation by vomitoxin (deoxynivalenol) in vitro and in vivo. Toxicol Appl Pharmacol 2003;187:80–8.
31. Azcona-Olivera JI, Ouyang Y, Murtha J, Chu FS, Pestka JJ. Induction of cytokine mRNAs in mice after oral exposure to the trichothecene vomitoxin (deoxynivalenol): relationship to toxin distribution and protein synthesis inhibition. Toxicol Appl Pharmacol 1995;133:109–20.
32. Moolenbeek C, Ruitenberg EJ. The "Swiss roll": a simple technique for histological studies of the rodent intestine. Lab Anim 1981;15:57–9.
33. Kostic AD, Xavier RJ, Gevers D. The microbiome in inflammatory bowel disease: current status and the future ahead. Gastroenterology 2014;146:1489–99.
34. Maresca M, Fantini J. Some food-associated mycotoxins as potential risk factors in humans predisposed to chronic intestinal inflammatory diseases. Toxicon 2010;56:282–94.
35. Van De Walle J, Romier B, Larondelle Y, Schneider YJ. Influence of deoxynivalenol on NF-κB activation and IL-8 secretion in human intestinal Caco-2 cells. Toxicol Lett 2008;177:205–14.
36. Sobrova P, Adam V, Vasatkova A, Beklova M, Zeman L, Kizek R. Deoxynivalenol and its toxicity. Interdiscip Toxicol 2010;3:94–9.
37. Wang Z, Wu Q, Kuca K, Dohnal V, Tian Z. Deoxynivalenol: signaling pathways and human exposure risk assessment—an update. Arch Toxicol 2014;88:1915–28.
38. Gnoth MJ, Rudloff S, Kunz C, Kinne RK. Investigations of the in vitro transport of human milk oligosaccharides by a Caco-2 monolayer using a novel high performance liquid chromatography-mass spectrometry technique. J Biol Chem 2001;276:34363–70.
39. Eiwegger T, Stahl B, Haidl P, Schmitt J, Boehm G, Dehlink E, Urbanek R, Szepfalusi Z. Prebiotic oligosaccharides: in vitro evidence for gastrointestinal epithelial transfer and immunomodulatory properties. Pediatr Allergy Immunol 2010;21:1179–88.
40. Goehring KC, Kennedy AD, Prieto PA, Buck RH. Direct evidence for the presence of human milk oligosaccharides in the circulation of breastfed infants. PLoS ONE 2014;9:e101692.
41. De Walle JV, Sergent T, Piront N, Toussaint O, Schneider YJ, Larondelle Y. Deoxynivalenol affects in vitro intestinal epithelial cell barrier integrity through inhibition of protein synthesis. Toxicol Appl Pharmacol 2010;245:291–8.
42. Azcona-Olivera JI, Ouyang YL, Warner RL, Linz JE, Pestka JJ. Effects of vomitoxin (deoxynivalenol) and cycloheximide on IL-2, 4, 5 and 6 secretion and mRNA levels in murine CD4+ cells. Food Chem Toxicol 1995;33:433–41.

43. Pinton P, Braicu C, Nougayrede JP, Laffitte J, Taranu I, Oswald IP. Deoxynivalenol impairs porcine intestinal barrier function and decreases the protein expression of claudin-4 through a mitogen-activated protein kinase-dependent mechanism. J Nutr 2010;140:1956–62.
44. Pinton P, Nougayrede JP, Del Rio JC, Moreno C, Marin DE, Ferrier L, Bracarense AP, Kolf-Clauw M, Oswald IP. The food contaminant deoxynivalenol decreases intestinal barrier permeability and reduces claudin expression. Toxicol Appl Pharmacol 2009;237:41–8.
45. Rahner C, Mitic LL, Anderson JM. Heterogeneity in expression and subcellular localization of claudins 2, 3, 4, and 5 in the rat liver, pancreas, and gut. Gastroenterology 2001;120:411–22.
46. Patel RM, Myers LS, Kurundkar AR, Maheshwari A, Nusrat A, Lin PW. Probiotic bacteria induce maturation of intestinal claudin 3 expression and barrier function. Am J Pathol 2012;180:626–35.
47. Milatz S, Krug SM, Rosenthal R, Gunzel D, Muller D, Schulzke JD, Amasheh S, Fromm M. Claudin-3 acts as a sealing component of the tight junction for ions of either charge and uncharged solutes. Biochim Biophys Acta 2010;1798:2048–57.
48. Günzel D, Yu AS. Claudins and the modulation of tight junction permeability. Physiol Rev 2013;93:525–69.
49. Pastorelli L, De Salvo C, Mercado JR, Vecchi M, Pizarro TT. Central role of the gut epithelial barrier in the pathogenesis of chronic intestinal inflammation: lessons learned from animal models and human genetics. Front Immunol 2013;4:280.
50. Mantis NJ, Rol N, Corthesy B. Secretory IgA's complex roles in immunity and mucosal homeostasis in the gut. Mucosal Immunol 2011;4:603–11.
51. Johansson ME, Ambort D, Pelaseyed T, Schutte A, Gustafsson JK, Ermund A, Subramani DB, Holmen-Larsson JM, Thomsson KA, Bergstrom JH, et al. Composition and functional role of the mucus layers in the intestine. Cell Mol Life Sci 2011;68:3635–41.
52. Kim YS, Ho SB. Intestinal goblet cells and mucins in health and disease: recent insights and progress. Curr Gastroenterol Rep 2010;12:319–30.
53. Bracarense AP, Lucioli J, Grenier B, Drociunas Pacheco G, Moll WD, Schatzmayr G, Oswald IP. Chronic ingestion of deoxynivalenol and fumonisin, alone or in interaction, induces morphological and immunological changes in the intestine of piglets. Br J Nutr 2012;107:1776–86.
54. Zenhom M, Hyder A, de Vrese M, Heller KJ, Roeder T, Schrezenmeir J. Prebiotic oligosaccharides reduce proinflammatory cytokines in intestinal Caco-2 cells via activation of PPARγ and peptidoglycan recognition protein 3. J Nutr 2011;141:971–7.
55. Rossi O, Karczewski J, Stolte EH, Brummer RJ, van Nieuwenhoven MA, Meijerink M, van Neerven JR, van Ijzendoorn SC, van Baarlen P, Wells JM. Vectorial secretion of interleukin-8 mediates autocrine signalling in intestinal epithelial cells via apically located CXCR1. BMC Res Notes 2013;6:431.
56. Fusunyan RD, Quinn JJ, Ohno Y, MacDermott RP, Sanderson IR. Butyrate enhances interleukin (IL)-8 secretion by intestinal epithelial cells in response to IL-1beta and lipopolysaccharide. Pediatr Res 1998;43:84–90.
57. Keshavarzian A, Fusunyan RD, Jacyno M, Winship D, MacDermott RP, Sanderson IR. Increased interleukin-8 (IL-8) in rectal dialysate from patients with ulcerative colitis: evidence for a biological role for IL-8 in inflammation of the colon. Am J Gastroenterol 1999;94:704–12.
58. Sturm A, Baumgart DC, d'Heureuse JH, Hotz A, Wiedenmann B, Dignass AU. CXCL8 modulates human intestinal epithelial cells through a CXCR1 dependent pathway. Cytokine 2005;29:42–8.
59. Ortega-González M, Ocon B, Romero-Calvo I, Anzola A, Guadix E, Zarzuelo A, Suarez MD, Sanchez de Medina F, Martinez-Augustin O. Nondigestible oligosaccharides exert nonprebiotic effects on intestinal epithelial cells enhancing the immune response via activation of TLR4-NFκB. Mol Nutr Food Res 2014;58:384–93.
60. Vos AP, Haarman M, Buco A, Govers M, Knol J, Garssen J, Stahl B, Boehm G, M'Rabet L. A specific prebiotic oligosaccharide mixture stimulates delayed-type hypersensitivity in a murine influenza vaccination model. Int Immunopharmacol 2006;6:1277–86.
61. de Kivit S, Saeland E, Kraneveld AD, van de Kant HJ, Schouten B, van Esch BC, Knol J, Sprikkelman AB, van der Aa LB, Knippels LM, et al. Galectin-9 induced by dietary synbiotics is involved in suppression of allergic symptoms in mice and humans. Allergy 2012;67:343–52.
62. de Kivit S, Kraneveld AD, Knippels LM, van Kooyk Y, Garssen J, Willemsen LE. Intestinal epithelium-derived galectin-9 is involved in the immunomodulating effects of nondigestible oligosaccharides. J Innate Immun 2013;5:625–38.
63. Sagar S, Vos AP, Morgan ME, Garssen J, Georgiou NA, Boon L, Kraneveld AD, Folkerts G. The combination of Bifidobacterium breve with non-digestible oligosaccharides suppresses airway inflammation in a murine model for chronic asthma. Biochim Biophys Acta 2014;1842:573–83.
64. Villanacci V, Ceppa P, Tavani E, Vindigni C, Volta U. Coeliac disease: the histology report. Dig Liver Dis 2011;43(Suppl 4):S385–95.
65. Dickson BC, Streutker CJ, Chetty R. Coeliac disease: an update for pathologists. J Clin Pathol 2006;59:1008–16.
66. Pironi L, Bonvicini F, Gionchetti P, D'Errico A, Rizzello F, Corsini C, Foroni L, Gallinella G. Parvovirus b19 infection localized in the intestinal mucosa and associated with severe inflammatory bowel disease. J Clin Microbiol 2009;47:1591–5.